nature communications

Article

https://doi.org/10.1038/s41467-025-58571-2

Universal law of hierarchical dynamics in gels arising from confluence of local physically dynamic bonds

Received: 5 December 2024

Accepted: 21 March 2025

Published online: 05 April 2025

Check for updates

Yi Hui Zhao[1,2], Yu Sen Jie[1,2], You Cai Xue[1,2], Zi Wei Shi[2,3], Yuan Chen Dong[2,3], Murugappan Muthukumar[4] ✉ & Di Jia[1,2] ✉

Gels comprised of dynamic bonds are important candidates for the emerging 'intelligent' gels due to their unique characteristics. We report a universal law of hierarchical gel dynamics arising from association-dissociation of physical crosslinks, as discerned from dynamic light scattering (DLS) on diverse sets of complex gels. It is the first experimental evidence of a stretched exponential decay with a universal exponent 1/3 in DLS for all the physical gels, complementing more than five decades of DLS studies on conventional chemical gels. Here we show that diversely different chemistries of dynamic bonds map into the observed unifying law for large-scale collective dynamical properties of physical gels. This discovery allows identification of whether physical or chemical bonds dominate the crosslinks in complex gels, as well as extraction of local energetics of the constituent physical crosslinks by their characteristic relaxation times. It also elicits large-scale functional properties applicable in smart gels.

Dynamically adaptable 'intelligent' gels are emerging as a new class of materials in numerous fields due to their attributes such as time-programmable, self-healing, recycling, and adhesive properties[1–5], with mimicry of human organs, tissues, and even brain[6,7]. These properties are in contrast with the rubbery properties of the well-trodden chemical gels formed with only covalent crosslinks. In general, dynamical gels are hybrids formed by both chemical crosslinks and physically associating crosslinks. The physical dynamical bonds act as sacrificial bonds by reversibly breaking and reforming to dissipate energy to protect the elastic attributes of the covalently crosslinked network. The coexistence of these two kinds of crosslinks, with a dominance of dynamical bonds, is central to mimicking self-healing properties of biological systems and applications such as electronic skins and soft robotics[8–14].

The physical dynamic bonds encompass a broad variety, including hydrogen bonding, electrostatic interaction, hydrophobic association, π-π stacking, coordination complex formation, etc refs. 2,3. (Fig. 1). The binding energies of such physical bonds are relatively low (less than 300 kJ/mol) in comparison with those of covalent bonds in the chemically crosslinked gels[15–17] (Fig. 1). Despite their weak binding energy, the physical dynamic bonds are indispensable to biological systems[18–22]. The higher-order structures, functionality, and phase behaviors of aggregates of various biological macromolecules, such as intrinsically disordered proteins and unregulated disease onset, all depend on the collective behaviors of dynamic bonds[23–25]. Contrasting the irreversible permanent structures created by chemical crosslinks, the reversible physical crosslinks endow the gels with dynamic homeostasis by facilitating easy structural adjustments and repair upon demand. These facile features are the root cause of the above-mentioned broad spectrum of extraordinary properties exhibited by the diverse class of reversible physical gels. Therefore, for complex gel materials containing both chemical and physical bonds, it is imperative to assess whether physical dynamic crosslinks or chemical covalent crosslinks play the

[1]State Key Laboratory of Polymer Physics and Chemistry, Beijing National Laboratory for Molecular Sciences, Institute of Chemistry, Chinese Academy of Sciences, Beijing, China. [2]University of Chinese Academy of Sciences, Beijing, China. [3]CAS Key Laboratory of Colloid, Interface and Chemical Thermodynamics, Beijing National Laboratory for Molecular Sciences, Institute of Chemistry, Chinese Academy of Sciences, Beijing, China. [4]Department of Polymer Science and Engineering, University of Massachusetts Amherst, Amherst, Massachusetts, USA. ✉e-mail: muthu@polysci.umass.edu; jiadi11@iccas.ac.cn

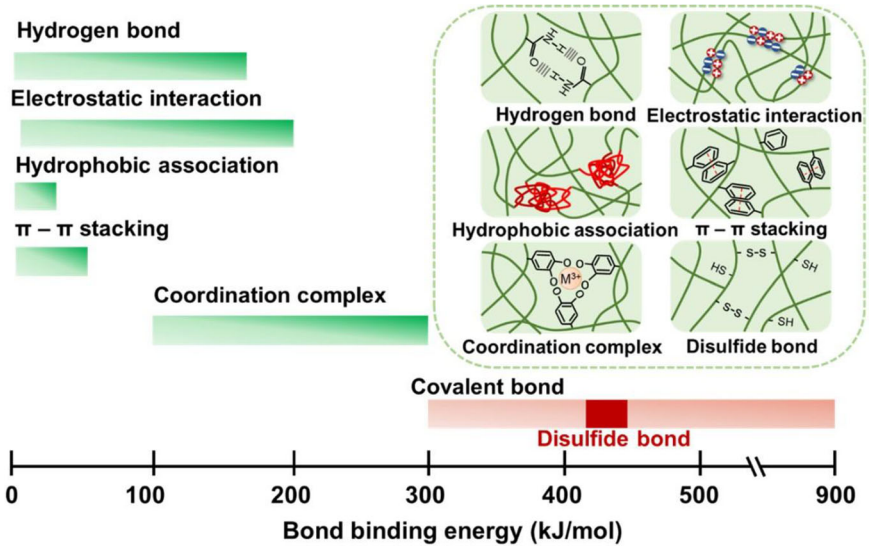

Fig. 1 | Bond binding energy map and schematic illustration of various bonds in gels. Binding energy map for various physical dynamic bonds and chemical covalent bonds[2,3,15–17]. Different types of bonds in gel networks are schematically illustrated.

dominant role in the gel, as well as to quantify the binding energy of these physical dynamic crosslinks.

It is natural to expect the overall dynamics of physical gels to be faithful and unique representations of the above-mentioned specifics of the chemical details of dynamic crosslinks. In contrast, we report a discovery of a universal law of gel dynamics applicable to all physical dynamic gels, and identification of whether physical dynamic bonds or chemical covalent bonds dominate in the hybrid gels, independent of their specific chemical nature.

Results

Universal law of hierarchical dynamics for physical gels

While investigating the dynamics of various types of physical gels with distinctly different physical crosslinks, such as hydrogen bonds, ionic bonds, and hydrophobic interactions, *etc*. (Fig. 2a), we serendipitously discovered that all these gels exhibited a new universal hierarchical dynamics, which is entirely different from the well-known results on chemical gels. In our experiments, we used the dynamic light scattering (DLS) technique which is most suited to explore the internal dynamics and elasticity of gels. In DLS, by measuring the scattered light intensity-intensity correlation function in terms of the decay time t at different scattering wavevectors $q = (4\pi/\lambda)\sin(\theta/2)$ (λ is the wavelength of the incident light, and θ is the scattering angle, Fig. 2b), and using the Siegert relation[26], the normalized electric field-field correlation function $g_1(q, t)$ is obtained. For all kinds of chemical gels, $g_1(q, t)$ is proportional to the time correlation function of the end-to-end distance vector $\mathbf{X}_m(t)$ of the polymer strand with m monomers between two adjacent crosslinks (Fig. 2b). As well-established in the literature over five decades for chemically crosslinked gels[27–36], $g_1(q, t)$ obeys an exponential decay with the relaxation rate $\Gamma = D_{gel}\, q^2$ [31,32], with the gel diffusion coefficient D_{gel} representing the gel elasticity (Methods) and the relaxation rate Γ representing inverse relaxation time,

$$g_1(q,t) = \langle \mathbf{X}_m(t) \cdot \mathbf{X}_m(0) \rangle = e^{-\Gamma t} = e^{-D_{gel} q^2 t} \text{(chemical gels)} \qquad (1)$$

Generally, if $g_1(q, t)$ follows exponential decay with time and obeys $\Gamma = Dq^2$, then it is a diffusive mode with the diffusion coefficient D[31,32]. As a reference point, our DLS results on the well-studied chemically crosslinked poly(acrylamide) (PAM) gels with 1% crosslink density are consistent with the above purely single exponential decay of $g_1(q, t)$ (Fig. 2c). From the relaxation times Γ measured at multiple scattering angles, the gel diffusion coefficient $D_{gel} = 4.88 \times 10^{-7}\text{cm}^2/\text{s}$ can be obtained from the slope of Γ / q^2 (Supplementary Fig. 1a).

On the other hand, in stark contrast with the standard behavior of Fig. 2c and as depicted in Fig. 2d–f, in addition to the diffusive exponential decay with D_{gel} representing the gel elasticity, all three types of physical gels also exhibit a stretched exponential decay of $g_1(q, t)$ according to

$$g_1(q,t) = e^{-(\frac{t}{\tau_\beta})^\beta} \quad \beta = \frac{1}{3} \text{(physical gel; universal)} \qquad (2)$$

where the stretched exponential exponent β is a universal constant 1/3 for all three physical gels, and the characteristic relaxation time τ_β is specific to the particular gel. The significantly lowered value of $\beta = 1/3$, compared to $\beta = 1$ for chemical gels (Eq. (1)), and the much longer times associated with τ_β, compared to relaxation times of the gel mode with D_{gel}, emphasize that many dynamical modes associated with internal chain relaxations are coupled and effectively function as hierarchical relaxations. This stretched exponential mode representing hierarchical dynamics is well decoupled with the inevitable gel mode, with D_{gel} representing the gel elasticity.

In terms of details, Fig. 2d corresponds to the first type of hydrogen-bond-driven physical gels, namely, poly(acrylamide) physical gels without any chemical crosslinkers. The correlation function $g_1(q, t)$ of this gel can be uniquely fitted by one exponential decay and one stretched exponential decay (the fitting function is at the top of the figure). The quality of the fitting curve (red line) with the raw experimental data (black squares) is excellent, as evident from the zero residuals (blue triangles). The first exponential mode is the gel mode with diffusion coefficient $D_{gel} = 5.87 \times 10^{-7}$ cm^2/s obtained from the slope of Γ / q^2 measured at multiple scattering angles (Supplementary Fig. 1b), which is similar to that obtained in the covalently crosslinked PAM gels (Supplementary Fig. 1a). The second mode of stretched exponential decay is non-diffusive since the relaxation rates Γ measured at all angles are not proportional to q^2 (Supplementary Fig. 1c). The stretched exponent β is independent of the scattering angles (Supplementary Fig. 1d) and the averaged β value is $\beta = (0.33 \pm 0.03)$. Such a non-diffusive stretched exponential mode for PAM physical gels without chemical crosslinkers represents the dissociation-association hierarchical relaxations of the reversible physical crosslinks composed of hydrogen bonds. This is the first experimental evidence of the occurrence of the stretched exponential mode in DLS for

https://doi.org/10.1038/s41467-025-58571-2

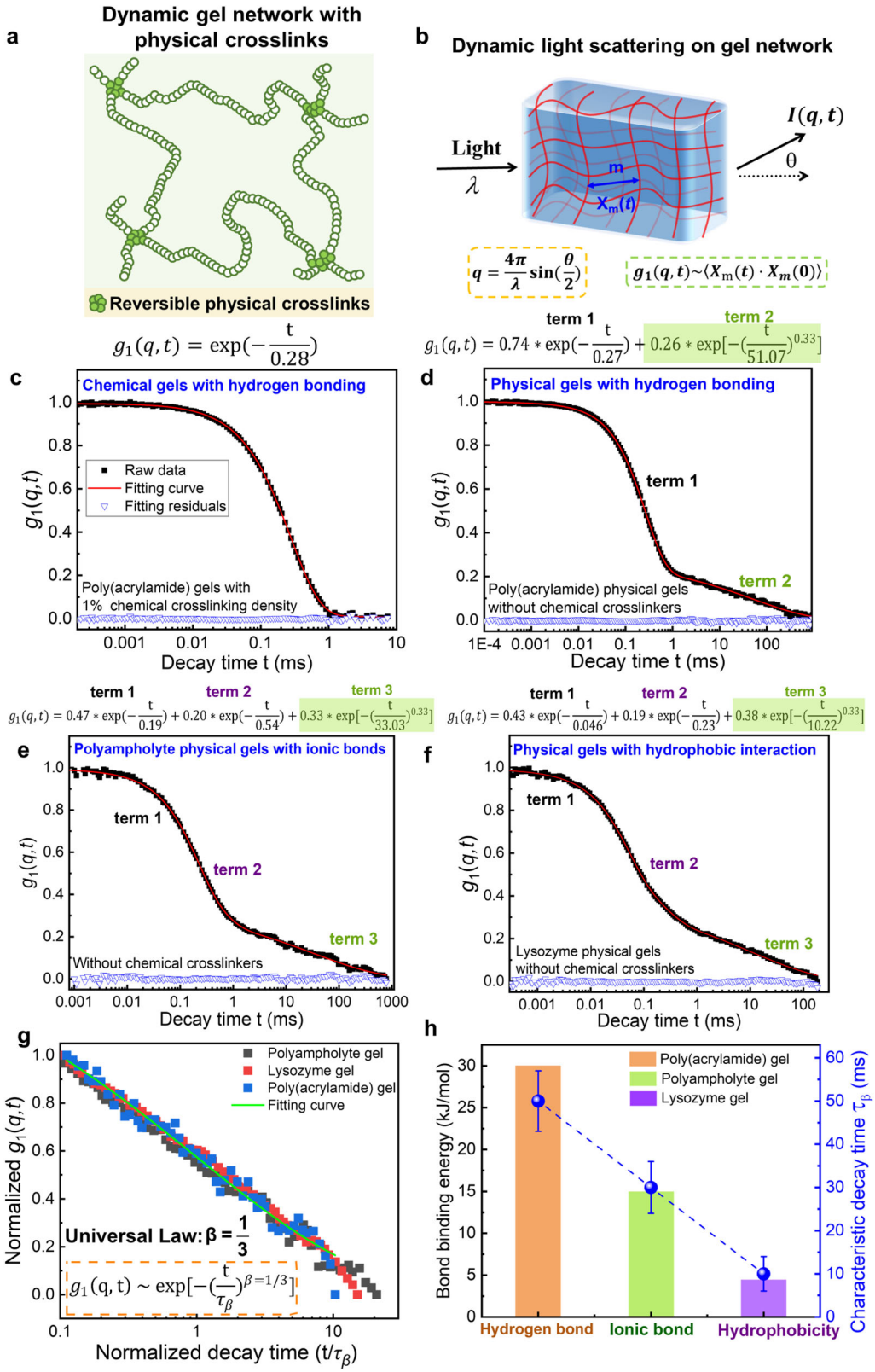

polyacrylamide gels since the first DLS measurement was conducted on polyacrylamide gels in 1973[27].

The second type investigated here is electrostatically driven polyampholyte gels with ionic bonds in the crosslinks, without any chemical crosslinks. In these gels, cationic monomers and anionic monomers are randomly distributed along the gel strands with a stoichiometric charge ratio[8]. The $g_1(q, t)$ of polyampholyte physical gels (Fig. 2e) can be fitted by three modes, with the presence of the non-diffusive stretched exponential decay with the averaged stretched exponent $\beta = 0.33 \pm 0.03$ (Fig. 2e and Supplementary Fig. 2b, c), representing the dissociation-association hierarchical relaxations of the reversible physical crosslinks composed of ionic bonds. The other two exponential modes are diffusive with the first mode being the gel mode representing gel elasticity with $D_1 = D_{gel} = 7.19 \times 10^{-7}$ cm^2/s

Fig. 2 | Dynamic light scattering results for various types of physical gels exhibiting universal hierarchical gel dynamics with unique stretched exponent $\beta = 1/3$. **a** Cartoon of a general dynamic gel network with physical crosslinks. **b** Basic principle of DLS technique on a gel network. **c**–**f** Correlation function $g_1(q, t)$ measured by DLS at scattering angle 30° for various gels and their corresponding best fitting functions (at the top) for the fitting curve (red line) to the raw data (black squares) with fitting residuals (blue triangles) for poly(acrylamide) gel with 1% chemical crosslinking density, as a reference system (**c**), poly(acrylamide) physical gel without chemical crosslinkers assembled by hydrogen bonds (**d**), polyampholyte physical gel of poly (sodium 4-vinylbenzenesulfonate-co-3-(methacryloylamino) propyl-trimethylammonium chloride) with ionic bonds at stoichiometric charge ratio $r = 0.52$ (number of negatively charged groups to the total number of charged groups) without chemical crosslinkers dialyzed against 2 M NaCl solutions (**e**), and lysozyme protein physical gel assembled by hydrophobic associations without chemical crosslinkers (**f**). **g** Superposition of normalized correlation function $g_1(q, t)$ as a plot against the decay time in units of the characteristic relaxation time τ_β at scattering angle 30° for three types of physical gels in (**d**–**f**), all with universal law of stretched exponent $\beta = 1/3$. **h** Correlation between the measured characteristic relaxation time τ_β (filled circles, right axis) and the specific bond binding energy (bars, left axis) obtained from literature[42–45] for the three types of physical gels in (**d**–**f**). Error bars reflect the standard deviation from measurements of three different spatial locations within three replicate gel samples.

(Supplementary Fig. 2a), which is in the same order of magnitude of D_{gel} for the chemical crosslinked polyampholyte gels (Supplementary Fig. 5c). The second mode is attributed to the "salt ion mode" corresponding to the coupled motion of the co-ions and counterions with polyampholyte backbones[37,38] with $D_2 = 2 \times 10^{-7}$ cm^2/s. (Supplementary Fig. 2a). Such a "salt ion mode" would disappear when the salt concentration in the gel is very low (Supplementary Fig. 5c).

The third type of physical gels is the natural lysozyme fibrillar gel networks with hydrophobic associations in the crosslinks without chemical crosslinks synthesized by following Miller's method[39–41] (Supplementary Fig. 3a and Supplementary Materials and Methods). Like the other two types of physical gels, $g_1(q, t)$ of lysozyme physical gels also have the non-diffusive stretched exponential decay with stretched exponent $\beta = 0.33$ (Fig. 2f and Supplementary Fig. 3c, d), indicating the dissociation-association hierarchical relaxations of the hydrophobic interaction-driven physical crosslinks. For the other two diffusive modes, the second mode is the gel mode with $D_2 = D_{gel} = 5.16 \times 10^{-7}$ cm^2/s, and the first mode is the "salt ion mode" with $D_1 = 3.28 \times 10^{-6}$cm^2/s (Supplementary Fig. 3b) due to their salt concentration dependence. As salt concentration increases from 0 to 0.1 M, D_1 increases three times to 9.67×10^{-6} cm^2/s (Supplementary Table 1), which is close to the diffusion coefficient of the coupled motion between the counterion and polyelectrolyte backbone in solutions[37,38], thus D_1 is the "salt ion mode". While D_2 is salt-independent, and its value is in the same order of magnitude of D_{gel} for chemical gels (Supplementary Table. 1). Thus, D_2 is the gel mode representing gel elasticity for lysozyme fibrillar gels.

As depicted in the universal plot of Fig. 2g, the normalized stretched exponential decay term in $g_1(q, t)$ for various types of physical gels, including hydrophobic association-driven lysozyme gels, ionic bond-driven polyampholyte gels, and hydrogen bonding-driven polyacrylamide gels can all superpose into a single master curve of stretched exponential decay with a universal stretched exponent $\beta = 1/3$ (Eq. (2)). This demonstrates that the specific local dynamic bonding equilibria converge into a single hierarchical dynamical mode that is universal to all physical gels, independent of significant differences in their chemical makeup. The local chemical nature of the reversible physical crosslinks appears only in the characteristic relaxation time τ_β setting the time scale of hierarchical dynamics in the stretched exponential decay. τ_β originating from the dissociation-association equilibria of the dynamic physical crosslinks is exponentially correlated with the free energy (ϵ) of physical crosslink formation. Therefore, larger binding energy leads to longer characteristic relaxation time τ_β, while the value of β is a constant at 1/3. The correlation between the measured characteristic relaxation time τ_β for hierarchical dynamics and the bond binding energy is shown in Fig. 2h. For the three types of bonds investigated here, the hydrogen bond binding energy between amide groups is around 30 kJ/mol[42] with the measured $\tau_\beta = 51.1$ ms, the ionic bond binding energy between sulfonate groups and ammonium groups is 15 kJ/mol[43] with the measured $\tau_\beta = 30.0$ ms, and the hydrophobic bond binding energy of lysozyme proteins is 4.4 kJ/mol[44,45] with the measured $\tau_\beta = 10.2$ ms. Thus, higher bond binding energy at the local level leads to longer characteristic relaxation time τ_β for the large-scale hierarchical dynamics.

Now that we have discovered a universal dynamical law detected by DLS to quickly identify physical dynamic gels versus chemical covalent gels, it becomes obvious to ask the following questions:

(a) Is there a theoretical basis for this phenomenon based on sound polymer physics concepts?
(b) Once the theory is developed to explain the above DLS results, would the new theory and the universal hierarchical dynamics be applicable to more complex gels consisting of an ensemble of different kinds of dynamic bonds?

We address these questions in the affirmative, as detailed below.

Theory

To gain insight into the molecular origin and characteristics of the hierarchical dynamics of physical gels, and to rationalize the universal value $\beta = 1/3$ of the stretched exponent for $g_1(q, t)$, we develop the following arguments based on polymer physics concepts. Generic to all physical crosslink formation, the two key quantities that are unique to the association-dissociation of a physical crosslink are[46–48]: free energy gain ϵ and free energy barrier ϵ_a for association (Fig. 3a). Both ϵ and ϵ_a are specific to the particular physical bond. The rate of association k_a and the rate of dissociation k_d are $\tau_O^{-1} \exp(-\epsilon_a/k_BT)$ and $\tau_O^{-1} \exp(-(\epsilon_a + \epsilon)/k_BT)$, respectively, where k_BT is the Boltzmann constant times the temperature and τ_O is a microscopic monomeric time scale, depending on the monomer friction coefficient and temperature. The average lifetime of a monomer inside a crosslink is $\tau_b = \tau_O \exp((\epsilon + \epsilon_a) / k_BT)$.

The inherent characteristic of reversible dynamic gels is the perpetual rearrangement of the connectivity of the polymer network by executing association-dissociation of the various physical crosslinks (Fig. 3b). As a result, the physical crosslinks are constantly changing due to their dynamic and reversible nature. Thus, the distribution of lengths of polymer strands between adjacent crosslinks is also constantly changing. According to the standard statistical analysis of gelation, the contiguous number of monomers m that are not participating in any crosslink is polydisperse, given by the distribution function $P(m)$,

$$P(m) = k_a e^{-k_a m} \tag{3}$$

where k_a is the rate of crosslink formation. Each strand with a particular value of m exhibits its chain dynamics. Since m is polydisperse, the internal dynamics of the physical gel is a superposition of the dynamics of all strands with various values of m allowed by Eq. (3).

Let us consider a labeled chain of N monomers, out of which N_c monomers are involved in dynamic crosslinks and (N-N_c) monomers are free from crosslinks. Its chain dynamics is equivalent to that of a random copolymer, where the friction coefficient ζ_c of a monomer inside a reversible physical crosslink is $\zeta_O \exp((\epsilon + \epsilon_a)/k_BT)$, with ζ_O being the friction coefficient of a monomer in its un-crosslinked state.

https://doi.org/10.1038/s41467-025-58571-2

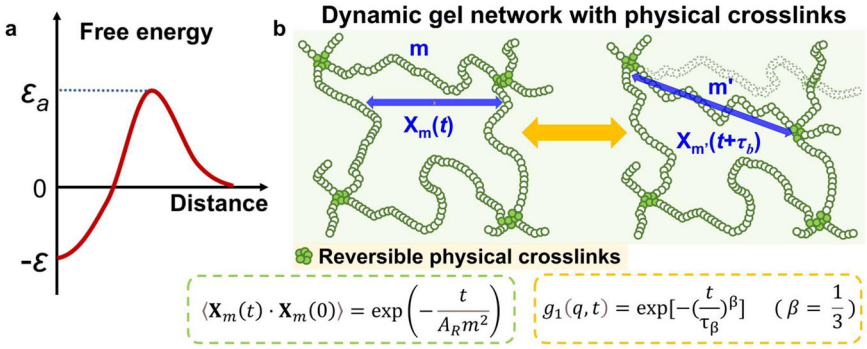

Fig. 3 | Mechanism of association-dissociation hierarchical dynamics for reversible dynamic gels with physical crosslinks. a Free energy profile of the association of two monomers as a function of separation distance. ϵ and ϵ_a are the free energy gain and free energy barrier for pair formation. **b** Monomers involved in dynamic crosslinks and monomers free from crosslinks within the gel strands are schematically illustrated. The strand with m number of monomers and end-to-end distance $\mathbf{X}_m(t)$ changes to m' and $\mathbf{X}_{m'}(t+\tau_b)$ after an elapse of lifetime τ_b of a physical bond, causing the perpetual change in the population of polydisperse strands.

Since the experimental conditions of our gels are in semidilute conditions, where hydrodynamic interaction is screened, and entanglement effects are weak, the Rouse dynamics with Gaussian chain statistics for the strands is appropriate[49,50]. The longest relaxation time (τ_{Rouse}) for a random copolymer of N monomers obeying Rouse dynamics is

$$\tau_{Rouse} = A_R N^2 \tag{4}$$

where A_R depends on the physical crosslink density ρ_c, ϵ, ϵ_a, and ζ_o (Methods). According to the theory of polymer dynamics, the time correlation function of the end-to-end distance vector $\mathbf{X}_m(t)$ of a Rouse strand with m monomers is[49,51,52]

$$\langle \mathbf{X}_m(t) \cdot \mathbf{X}_m(0) \rangle = \exp\left(-\frac{t}{A_R m^2}\right) \tag{5}$$

where A_R is given in Eq. (4). According to the theories of light scattering and gel elasticity[27,53], $g_1(q, t)$ is a superposition of $\langle \mathbf{X}_m(t) \cdot \mathbf{X}_m(0) \rangle$ for each m weighted by the polydispersity distribution $P(m)$,

$$g_1(t) \sim \int dm\, P(m) \langle \mathbf{X}_m(t) \cdot \mathbf{X}_m(0) \rangle \tag{6}$$

Using Eqs. (3)–(5) and performing the integral in Eq. (6), we obtain the universal law of Eq. (2) with $\beta = 1/3$ and (Methods)

$$g_1(q,t) = e^{-(\frac{t}{\tau_\beta})^\beta} \beta = \frac{1}{3}$$
$$\tau_\beta = \frac{4\tau_0}{27} e^{2\epsilon_a/k_B T} (e^{\frac{\epsilon+\epsilon_a}{k_B T}} \rho_c + (1-\rho_c)). \tag{7}$$

Therefore, $\beta = 1/3$ is universal for all hierarchical dynamics of physical gels, and τ_β is the characteristic collective relaxation time unique to the specific gels.

Supported by the above conceptual advance on the onset and nature of hierarchical dynamics in physical dynamic gels, we have additionally found the universality of this new gel dynamics by deliberately arresting and tuning this phenomenon. Furthermore, we demonstrate below the universality of this phenomenon in both natural and synthetic complex gels with multiple simultaneous contributions from several kinds of dynamic bonds.

One-or-none principle of switching off hierarchical dynamics with chemical crosslinks

To explore the boundary of the universal dynamical law for the gels with physical / chemical crosslinks, poly(acrylamide) (PAM) gels with different chemical crosslinking densities of 0–0.5% are studied. As described before, PAM gel with 0% chemical crosslinking density is a physical gel obeying the hierarchical dynamics of non-diffusive stretched exponential decay (Fig. 2d), while PAM gel with 1% chemical crosslinking density is a chemical gel with the absence of the stretched exponential decay in DLS (Fig. 2c). As shown in Fig. 4a, for 0.1% chemical crosslinking density, the non-diffusive stretched exponential decay is again present with $\beta = 1/3$ (Supplementary Fig. 4a–d). Thus, for such a low permanent crosslink density as 0.1%, the native hierarchical dynamics arising from physical crosslinks is still maintained. Moreover, the fraction of the stretched exponential mode decreases from 23% to 9% as the chemical crosslinking density increases from 0 to 0.1% (Fig. 4a). On the other hand, when the chemical crosslinking density is 0.2% and above, the stretched exponential mode disappears, and $g_1(q, t)$ can be fitted only by a single exponential decay representing the gel elasticity (Fig. 4a and Supplementary Fig. 4e, f). Please note that the boundary of chemical crosslinking density for the occurrence of such hierarchical dynamics is system-dependent.

Therefore, the universal law of hierarchical dynamics can also be applied for weakly crosslinked chemical gels, in which the physical dynamic bonds dominate the crosslinks. For gels with high chemical crosslinking density where the permanent covalent bonds dominate the crosslinks, the hierarchical stretched exponential decay is totally averted. Thus, the response of the hierarchical dynamics of physical gels to additional chemical crosslinks obeys the 'one-or-none' principle. Simply by monitoring the presence/absence of the stretched exponential decay in DLS, we can evaluate whether the physical dynamic bonds or permanent covalent bonds dominate the crosslinks of complex gels containing both physical and chemical bonds in the crosslinks.

Tuning the hierarchical dynamics with conformational transition

We have also investigated the robustness of the universal hierarchical dynamics with respect to conformational transitions of the gel networks. A suitable system to monitor this feature is polyampholyte (PA) gels with ionic bonds because the ionic bond strength can be easily tuned by dialyzing against solutions of different NaCl concentration C_s. An example is given in Fig. 4b, where the correlation function $g_1(q, t)$ is presented for a PAgel with weak chemical crosslinking (0.5% chemical crosslinking density) and stoichiometric charge ratio $r = 0.52$[8] dialyzed

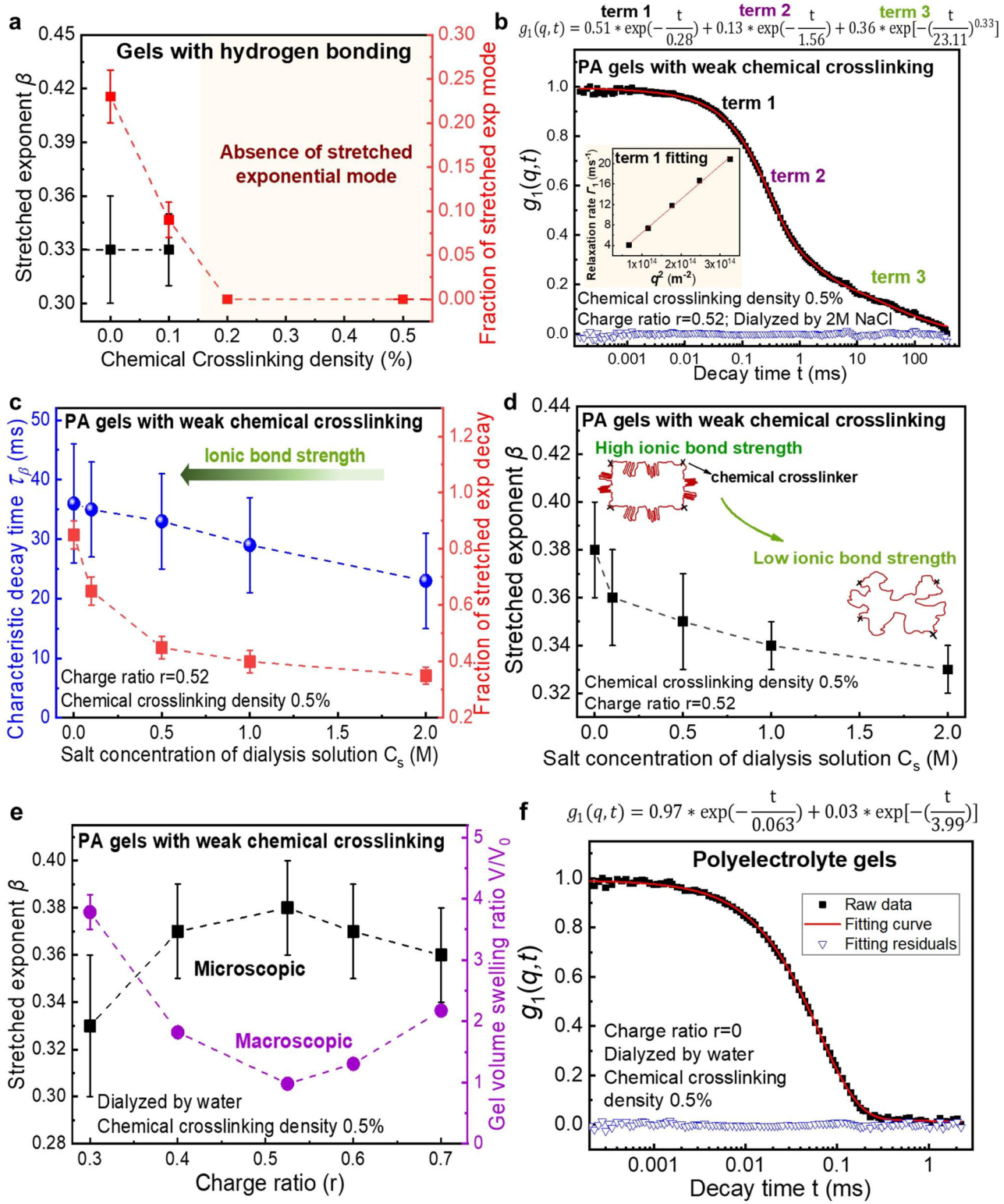

against 2 M NaCl. Analogous to the PA gel without any chemical crosslinks and at the same ionic bond strength (Fig. 2e), $g_1(q, t)$ can be fitted uniquely by two diffusive exponential decays and a non-diffusive stretched exponential decay with stretched exponent $\beta = 0.33$ (Fig. 4b and Supplementary Fig. 5a, b). The first mode is the gel mode with $D_1 = D_{gel} = 6.58 \times 10^{-7}$cm^2/s, and the second mode is the "salt ion mode" ($D_2 = 8.23 \times 10^{-8}$cm^2/s), which decreases with the decrease of salt concentration and finally disappears when the salt concentration is very low[37,38] (Supplementary Fig. 5c).

Notably, the characteristic relaxation time τ_β decreases almost by half as C_s increases from 0 to 2 M because the added salt screens the electrostatic interaction of the ionic bonds and accelerates the dissociation-association hierarchical relaxation of the physical crosslinks (Fig. 4c). Consistent with this screening effect, the fraction of the stretched exponential mode arising from the dissociation-association equilibria of the ionic bonds also decreases from 85% at $C_s = 0$ M to 35% at $C_s = 2$ M (Fig. 4c). Moreover, β values in the stretched exponential decay change slightly with conformational transition in the gel strands,

Fig. 4 | Hierarchical gel dynamics measured by DLS for weakly chemical crosslinked gels. a Physical gels to chemical gels transition identified by the presence/absence of the stretched exponential mode in DLS. The fraction of stretched exponential mode and the stretched exponent β as a plot of the chemical crosslinking density for poly(acrylamide) gels. **b** Correlation function $g_1(q, t)$ measured by DLS at scattering angle 30° for weakly chemical crosslinked polyampholyte (PA) gels with 0.5% chemical crosslinking density and charge ratio $r = 0.52$ (number of negatively charged groups to the total number of charged groups) after dialyzed by 2 M NaCl. The fitting function shown at the top are required for the best fit (red line) to the raw data (black squares) with fitting residuals (blue triangles). Inset is the fitting curve for term 1 of gel mode to obtain the gel diffusion coefficient $D_{gel} = 6.58 \times 10^{-7}$cm^2/s. **c** Characteristic relaxation time τ_β for stretched exponential mode at scattering angle 30° and the averaged fraction of the stretched exponential mode for weakly chemical crosslinked PA gels after dialyzing against NaCl solutions with different salt concentrations C_s. **d** Averaged stretched exponent β values of weakly chemical crosslinked PA gels after dialyzing against NaCl solutions at different salt concentrations with cartoons illustrated the conformational change of the gel strands. **e** Charge ratio dependence of microscopic β values and macroscopic gel volume swelling ratio V/V_O for weakly chemical crosslinked PA gels dialyzed by water (V_O denotes the gel volume in the as-prepared state, and V denotes the gel volume after swelling by water). **f** Correlation function $g_1(q, t)$ at scattering angle 30° and the corresponding fitting results for 100% positively charged polyelectrolyte gels with 0.5% chemical crosslinking density after dialyzed by water. Error bars reflect the standard deviation from measurements of three different spatial locations within three replicate gel samples.

but still keeping in a narrow range. In general, the stretched exponent β equals $1/(2\nu+2)$ with size exponent ν ("Methods"). When the salt concentration C_s is reduced, the electrostatic interaction is not fully screened, and hence more of the oppositely charged groups in the gel strands will complex together to eventually attain a shrunk strand with the size exponent $\nu \simeq 1/3$. Upon an increase in C_s, the gel strands expand to attain random-walk statistics with $\nu \simeq 1/2$, as schematically illustrated in the cartoons in Fig. 4d. As a result, the value of β decreases gradually from 3/8 ($\nu = 1/3$) at low C_s for relatively shrunk chain conformation to 1/3 ($\nu = 1/2$) at high C_s for Gaussian chain conformation (Fig. 4d).

To further validate the crossover behavior of β values with conformational transition, we have studied the role of charge ratio r (number of negatively charged monomers to the total number of charged monomers) of the PA gels dialyzed by water. Microscopically, at the stoichiometric charge ratio ($r = 0.52$), the β value reaches a maximum of 0.38 (while D_{gel} reaches a minimum (Supplementary Fig. 6a)), indicating that the gel network is in the shrunk state (Fig. 4e). When the charge ratio r deviates from the stoichiometric charge balance point on either side, β decreases because the gel strands are able to partially swell due to the unbalanced charges. On the other hand, the macroscopic gel volume swelling ratio V/V_O (where V_O is the volume of the as-prepared gel and V is the gel volume after dialysis against water) is the smallest at the stoichiometric charge ratio (Fig. 4e), consistent with the results of β and D_{gel} measured at the microscopic length scale. Both microscopic and macroscopic results demonstrate that the gel strands adopt the shrunk conformation at the stoichiometric charge ratio.

Lastly, when the charge ratio goes to the extreme of $r = 0$, the 100% positively charged polyelectrolyte gels dialyzed against water exhibit the normal DLS behavior of polyelectrolyte gels[31] of two exponential decays without the stretched exponential mode due to the lack of ionic bonds (Fig. 4f and Supplementary Fig. 6b, c). This result further demonstrates that the nature of stretched exponential decay arises from the dissociation-association equilibria of the dynamic ionic bonds in the crosslinks of the PAgels.

Validation of the universality of the hierarchical dynamical law on complex gels

In order to validate the universality and broad use of the newly discovered dynamical law in quickly identifying whether chemical covalent bonds or physical dynamic bonds dominate the crosslinks in complex gel materials, we have tested several natural and synthetic complex gels. Firstly, we have originally synthesized a new type of artificial mucus gel materials containing rich physical bonds, including hydrogen bonds, ionic bonds, hydrophobic association, π-π stacking, and also chemical crosslinking (Fig. 5a). Because of the unknown chemical conversion rate of the chemical crosslinkers, we cannot a priori tell whether chemical bonds or physical bonds dominate the crosslinks in the gel. Detected by DLS, the stretched exponential decay with $\beta = 1/3$ shows up in the correlation function $g_1(q, t)$, demonstrating that physical crosslinks dominate the complex artificial mucus gels, while the chemical crosslinking density is rather low (Fig. 5b, c and Supplementary Fig. 7a, b).

The second test is on self-assembled single-stranded DNA hydrogels constructed by complementary base pairing from Y-scaffolds and linkers[54] (Fig. 5d). The presence of the stretched exponential decay with $\beta = 1/3$ in the correlation function of DLS demonstrates that such a supramolecular self-assembled DNA gel is a physical gel mainly driven by van der Waals interactions and hydrogen bonds through base pairing (Fig. 5e, f and Supplementary Fig. 7c, d). We have also tested natural silk fibroin gels made from B. mori silkworm cocoons containing both physical crosslinks such as hydrophobic interaction and chemical covalent crosslinking with unknown chemical conversion rate due to the complexity of the gelation reaction[55]. Due to the absence of the stretched exponential decay in DLS, we can confidently conclude that the chemical covalent bonds dominate the crosslinks of the silk fibroin gels (Fig. 5g, h and Supplementary Fig. 7e). Lastly, hyaluronic acid gels with physical bonds of hydrogen bonding and electrostatic interaction, as well as cystamine chemical crosslinkers with unknown chemical conversion rate are also tested[31] (Fig. 5i). The correlation function can be fitted by one single exponential decay, demonstrating that it is a chemical gel in nature (Fig. 5j and Supplementary Fig. 7f).

With the test of various natural and synthetic complex gels, we conclude that the hierarchical dynamics of stretched exponential decay with $\beta = 1/3$ in DLS is a ubiquitous dynamical law and a key feature to identify whether chemical covalent bonds or physical dynamic bonds dominate the crosslinks of the gels. Please note that it is possible to have deviations from this law when additional effects are present. Based on Eq. (20), the stretched exponent is $\beta = 1/(2\nu+2)$ when the subchain dynamics obeys the Rouse dynamics. For Gaussian chain statistics with $\nu = 0.5$, we have $\beta = 1/3$. As an example of a deviation from this behavior, if the gel strands adopt molten-globule-like conformations with $\nu = 1/3$, then we have $\beta = 3/8$. In most cases, the gel strands have Gaussian chain statistics and obey Rouse dynamics, thus $\beta = 1/3$. It is, in principle, possible that the intra-strand excluded volume interactions and hydrodynamic interactions are not screened so that the exponent β could show a deviation[56] from $\beta = 1/3$.

Discussion

We have discovered a new universal hierarchical dynamical law of stretched exponential decay of fluctuations in gel elasticity, with the universal stretched exponent $\beta = 1/3$, detected by DLS on physical gels with diversely different chemical constituents. Moreover, the characteristic collective relaxation time τ_β in the stretched exponential mode is a measure of the local energetics of the physical crosslinks. This opens a possibility to design physical gel-based clocks, namely, structures and properties of complex gels such as time-programmable, self-healing, and recycling properties based on their characteristic relaxation time measured in DLS. We also report the boundary of the universal hierarchical dynamics by inducing its arrest with additional

https://doi.org/10.1038/s41467-025-58571-2

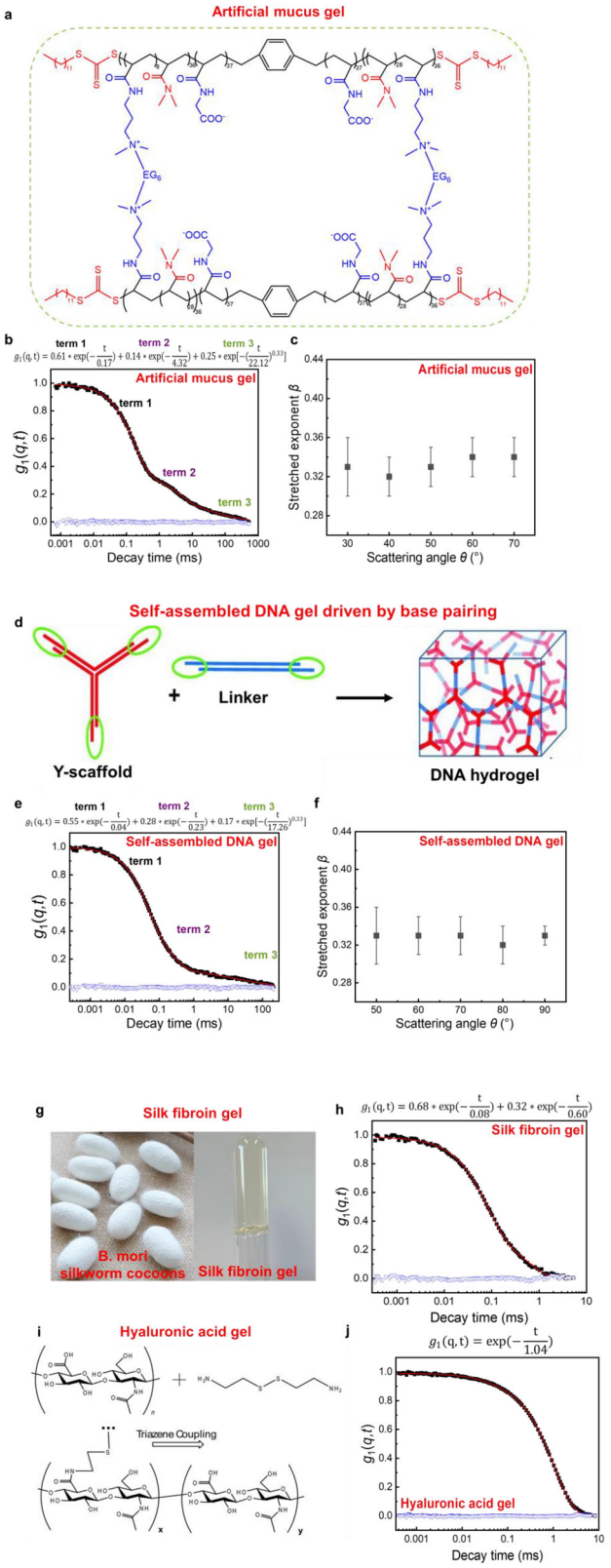

Fig. 5 | DLS tests and their fitting results of various natural and synthetic complex gels to verify the universality of the new dynamical law for physical gels. a Structure of artificial mucus gel. (Blue groups are relatively hydrophilic, and red groups are relatively hydrophobic). **b** Correlation function $g_1(q, t)$ measured by DLS and the corresponding fitting results for artificial mucus gel. **c** Stretched exponent β values at all scattering angles for artificial mucus gel. **d** Schematic illustration of the formation of self-assembled DNA gel driven by complementary base pairing[54]. Reproduced with permission from ref. 54. Copyright 2010, John Wiley and Sons. **e** Correlation function $g_1(q, t)$ measured by DLS and the corresponding fitting results for self-assembled DNA gel. **f** Stretched exponent β values at all scattering angles for self-assembled DNA gel. **g** Silk fibroin gel[55] from B. mori silkworm cocoons. **h** Correlation function $g_1(q, t)$ measured by DLS and the corresponding fitting results for silk fibroin gel. **i** Schematic illustration of the formation of hyaluronic acid gel[31]. Reproduced with permission from ref. 31. Copyright 2017, American Chemical Society. **j** Correlation function $g_1(q, t)$ measured by DLS and the corresponding fitting results for hyaluronic acid gel. Error bars reflect the standard deviation from measurements of three different spatial locations within three replicate gel samples.

covalent crosslinks and by tuning conformational changes in the gel strands.

It is well-known that such hierarchical dynamics are earmarks of traditional glasses observed in small molecular systems and alike at lower temperatures below their respective glass transition temperatures. In this context, it is remarkable that we have observed similar glass-like hierarchical dynamics in aqueous assemblies which contain mostly water and at room temperature. Since one of the main driving forces for this hierarchy in the present systems is conformational entropy, we may call the dynamic gels entropically diluted glasses. In view of this, one might ponder over whether there is an analog of the entropic driving force in traditional glasses at low temperatures, perhaps arising from orientational entropy and redistribution of cage effects. Thus, the present results open a new avenue to deeply get into the entropic attributes of free energy landscapes of even traditional glasses and the potential unification of glasses and gels into a single universality class.

Furthermore, in view of the validation of its universality in a broad variety of complex gels, the hierarchical dynamical law detected by DLS can provide a simple and general method to quickly identify whether physical dynamic bonds or chemical covalent bonds dominate the crosslinks of the gels. In addition, this procedure allows extraction of the effective local energetics of the reversible physical crosslinks in a large variety of complex gel materials, where several kinds of physical bonds can be concurrently dynamic. Quick identification of the dominance of physical bonds in composite gels enables the designable capability to tune several functional properties such as gel adhesion, phase transition in 3D printing, and memory in water-based memristors, as well as mimicry excellent properties in the natural systems such as hairy tongues of bats, mucus and mushy okra[57,58].

Methods

Theory of hierarchical gel dynamics

As depicted in Fig. 3a, the two key features characterizing crosslink formation are the free energy gain ϵ and the free energy barrier ϵ_a for pairwise association[46–48,56,59–61]. The rate of association k_a and the rate of dissociation k_d are $\tau_O^{-1}\exp(-\epsilon_a/k_BT)$ and $\tau_O^{-1}\exp(-(\epsilon_a+\epsilon)/k_BT)$, respectively, where k_BT is the Boltzmann constant times the temperature and τ_O is a microscopic monomeric time scale in the range of picosecond to nanosecond, depending on the monomer friction coefficient and temperature. The average lifetime of a monomer inside a crosslink is $\tau_b = \tau_O \exp((\epsilon+\epsilon_a)/k_BT)$ in the steady state.

In a system of volume V_O containing n primary chains, each with N monomers and monomer volume υ_O, the total number of monomers N_s capable of pairwise crosslinks is[56]

$$N_s = fnN = f\Phi_0 V_0/\upsilon_0 \tag{8}$$

where f ($\ll 1$) denotes the fraction of monomers with correct orientation required by chemical details for crosslink formation, and ϕ_O is the polymer volume fraction $nN\upsilon_O/V_O$. Using equilibrium statistical mechanics, the fraction of monomers q, associated into pairwise

crosslinks of free energy gain ϵ, is given by[56,59,60]

$$\frac{q}{(1-q)^2} = f\Phi_0 e^{\epsilon/k_BT} \tag{9}$$

As mentioned above, f is very small. In the simplest situation (without considering any free energy barriers for rotations), the value of f is 1/4π. This factor is further multiplied by the polymer volume fraction which in turn is also small. As a result, for moderate values of ϵ/k_BT, the factor q in the left-hand side of the above equation is very small. For such weak energy gains relevant to reversible gels, this reduces to

$$q \approx f\Phi_0 e^{\epsilon/k_BT} \tag{10}$$

The average number of pairwise crosslinks N_c per chain follows from Eqs. (8) and (10) as

$$N_c = \frac{1}{2}\frac{qN_s}{n} = \frac{1}{2}qfN = \frac{1}{2}f^2N\Phi_0 e^{\epsilon/k_BT} \tag{11}$$

where factor 2 arises from the requirement of two monomers to participate in a crosslink. The crosslink density ρ_c, defined as the fraction of crosslinked monomers in the system is N_c/N given by

$$\rho_c = \frac{1}{2}f^2\Phi_0 e^{\epsilon/k_BT} \tag{12}$$

Since $f \ll 1$ and $\phi_O < 1$, ρ_c is very small. For such weak crosslinking situations, the standard statistical analysis shows that the crosslinking along the chain backbone is a Poisson process[62,63]. Specifically, the contiguous number of monomers m that are not participating in any crosslink is polydisperse given by the distribution function $P(m)$,

$$P(m) = k_a e^{-k_a m} \tag{13}$$

where k_a is the rate of crosslink formation. Each strand with a particular value of m exhibits its chain dynamics. Since m is polydisperse, the internal dynamics of the physical gel is a superposition of the dynamics of all strands with various values of m allowed by Eq. (13).

Since N_c monomers of each labeled chain of N monomers are involved in dynamic crosslinks and (N-N_c) monomers are free from crosslinks, the chain dynamics is equivalent to that of a random copolymer, where the friction coefficient ζ_c of a monomer inside a reversible physical crosslink is $\zeta_O \exp((\epsilon+\epsilon_a)/k_BT)$, with ζ_O being the friction coefficient of a monomer in its un-crosslinked state. Furthermore, since $\phi_O \ll 1$ (corresponding to semidilute conditions, where hydrodynamic interaction is screened and entanglement effects are weak), the Rouse dynamics is appropriate for the present situation[49,50]. Furthermore, if the strands between crosslinks are not collapsed as in a poor solvent, the strands obey the Gaussian chain statistics with the size exponent $\nu = 1/2$. In such a situation, generally valid for reversible gels, the longest relaxation time (τ_{Rouse}) of a chain of N monomers is proportional to $N^{(2\nu+1)} \sim N^2$, with $\nu = 1/2$[49,50]. The longest relaxation time (τ_{Rouse}) for a random copolymer of N monomers with the fraction ρ_c (Eq. (12)) of monomers with friction coefficient ζ_c and the fraction (1−ρ_c) of monomers with friction coefficient ζ_O is given as[64]

$$\tau_{Rouse} = \tau_0(e^{\frac{\epsilon+\epsilon_a}{k_BT}}\rho_c + (1-\rho_c))N^2 \equiv A_R N^2 \tag{14}$$

where ρ_c is given in Eq. (12), τ_O absorbs monomer friction coefficient ζ_O and temperature, and A_R is as defined in this equation. According to the theory of polymer dynamics, the time correlation function of the end-to-end distance vector $\mathbf{X}_m(t)$ of a Rouse strand with m monomers is[49,51,52]

$$\langle \mathbf{X}_m(t)\cdot\mathbf{X}_m(0)\rangle = \exp\left(-\frac{t}{A_R m^2}\right) \tag{15}$$

where A_R is given in Eq. (14).

According to the theories of light scattering and gel elasticity[27,53], the time correlation function $g_1(q, t)$ is a superposition of $\langle \mathbf{X}_m(t)\cdot\mathbf{X}_m(0)\rangle$ for each m weighted by the polydispersity distribution $P(m)$,

$$g_1(t) \sim \int dm\, P(m)\langle \mathbf{X}_m(t)\cdot\mathbf{X}_m(0)\rangle \tag{16}$$

Substitution of Eqs. (13) and (15) in this equation yields,

$$g_1(t) \sim \int dm\, exp\left(-k_a m - \frac{t}{A_R m^2}\right) \tag{17}$$

Performing the integral using the saddle point approximation, we obtain

$$g_1(q,t) \sim \exp\left(-\left(\frac{t}{\tau_\beta}\right)^\beta\right)\ \beta = \frac{1}{3} \tag{18}$$

where

$$\tau_\beta = \frac{4\tau_0}{27}e^{2\epsilon_a/k_BT}(e^{\frac{\epsilon+\epsilon_a}{k_BT}}\rho_c + (1-\rho_c)) \tag{19}$$

Equation (18) exhibits the universality of the stretched exponential exponent $\beta = 1/3$, for the hierarchical internal dynamics of reversible physical gels independent of the local chemical nature of the reversible physical crosslinks, which appear only in the characteristic relaxation time τ_β setting the time scale of hierarchical dynamics. For example, for larger values of ϵ, τ_β is larger, but keeping the value of β at 1/3.

It is to be noted that the above conclusions are valid even if an additional small extent of covalent crosslinking (with rate k_c) is allowed in the reversible gelation process. In this case, k_a in Eq. (17) is replaced by ($k_a + k_c$). For higher values of k_c compared to k_a, deviations from the present universal law of $\beta = 1/3$ are expected, so much so that the hierarchical physical gel dynamics is averted. In the general case, where the strands can undergo conformational changes such that the size exponent is ν (for example, $\nu = 1/3$ if the gel strands adopt molten-globule-like conformations), the Rouse relaxation time in Eqs. (14) and (17) is proportional to $m^{2\nu+1}$, so that β follows as $1/(2\nu+2)$[51,56],

$$\beta = \frac{1}{2\nu+2} \tag{20}$$

Sample preparation and dynamic light scattering (DLS) measurement

The DLS tubes were washed with pure water and acetone separately more than three times. The tubes were dried in the oven overnight, and then we used aluminum foil to wrap them. Distilled acetone through an acetone fountain setup was used to clean up these tubes. Before polymerization, all the pre-gel solutions were filtered through a 220 nm PVDF hydrophilic filter into the tubes to remove the dust. The preparation of all the samples should be conducted in a super clean bench. DLS measurement was performed on a commercial spectrometer, which was equipped with a multi-τ digital time correlator (ALV/LSE-5004) using a wavelength of 532 nm laser light source. For each

sample, the scattering light intensity was correlated at scattering angles 30°, 40°, 50°, 60°, 70°, and 90° (Supplementary Fig. 8), and the range of wavevector q is from 8.1×10^6 m^{-1} to 2.2×10^7 m^{-1}. The relaxation time was averaged for three different spatial locations within three samples. Error bars reflect the standard deviation from measurements of three different spatial locations within three replicate gel samples.

Data acquisition and analysis

The scattering light intensity-intensity time correlation function $g_2(q, t)$ is measured by dynamic light scattering by means of a multi-channel digital correlator, and $g_2(q, t)$ is related to the normalized electric field correlation function $g_1(q, t)$ through the Siegert relation[26],

$$g_2(q,t) = \frac{<I(0)I(t)>}{<I>^2} - 1 = \beta\,|g_1(q,t)|^2 \tag{21}$$

where t is the decay time and $I(t)$ is the scattered light intensity, β is the instrument coherence factor.

For polymer solutions, $g_1(q, t)$ is proportional to the monomer density-density correlation expressed as ref. 26,

$$g_1(q,t) \sim <\rho(q,t)\rho(-q,0)> \sim e^{-\Gamma t} \tag{22}$$

If the dynamic mode is diffusive, then the relaxation rates Γ at multiple scattering angles are proportional to q^2, following $\Gamma = Dq^2$. From the slope of $\Gamma/\,q^2$, the diffusion coefficient D can be obtained. Based on the Stokes-Einstein equation $D = k_B\mathrm{T}/6\pi\eta R_h$ (where k_B is the Boltzmann constant, T is the temperature, η is the viscosity of the solution), the hydrodynamic radius R_h of the polymers can be obtained.

For chemically crosslinked gels, $g_1(q, t)$ is proportional to the time correlation function of the end-to-end distance vector $\mathbf{X}_m(t)$ of the polymer strands with m monomers between two adjacent crosslinks:

$$g_1(q,t) \sim \left\langle \mathbf{X}_m(t) \cdot \mathbf{X}_m(0) \right\rangle \sim e^{-\Gamma t} \tag{23}$$

As well-established in the literature over five decades for chemically crosslinked gels[27–36], $g_1(q, t)$ of gels depends on the modulus and the friction coefficient and also obeys an exponential decay with $\Gamma = D_{\mathrm{gel}}\,q^2$. Actually, nothing is diffusive in the gel networks, the gel diffusion coefficient D_{gel} indicates the gel elasticity with $D_{\mathrm{gel}} = M/f$, where M is the longitudinal modulus and f is the friction coefficient between the gel strands and the solvent. And the longitudinal modulus $M = K + 4/3\,G'$ is related to bulk modulus K and elastic modulus G'.

The electric field correlation function $g_1(q, t)$ can be fitted with a sum of several relaxation modes. The characteristic relaxation rate Γ_i was analyzed by using the CONTIN method[65] and multiple exponential fitting methods at each scattering angle. CONTIN method fits a weighted distribution of relaxation times and was first used to confirm multiple modes as,

$$g_2(q,t) - 1 = \int_0^\infty P(\Gamma)\exp(-\Gamma t)\,d\Gamma \tag{24}$$

where $P(\Gamma)$ is the weight of each relaxation rate Γ, as determined by an inverse Laplace transform.

For the multiple exponential fitting method, the correlation function $g_1(q, t)$ can be fitted by a sum of several exponential decays and a stretched exponential decay[51] as,

$$g_1(q,t) = \mathrm{a}_1 e^{-\Gamma_1 t} + \mathrm{a}_2 e^{-\Gamma_2 t} + a_3 e^{-(\Gamma_3 t)^\beta} \tag{25}$$

The function $g_1(q, t)$ was fitted by ORIGIN software, and the error between the raw data and the fitted function was minimized after iterations were performed. Iterations were performed until the best-fitting curve was obtained within the tolerance limit. Residuals of the difference between the fitted curve and the raw data are randomly distributed about the mean of zero, and the residuals do not have systematic fluctuations about their mean value.

Swelling methods

The as-prepared gel samples were dialyzed by deionized water or dialyzed against NaCl solution with different salt concentrations for a week. Specifically, for the polyampholyte physical gels without any chemical crosslinkers, Gong et al.'s previous studies show that when the ionic bond strength is high at low salt concentration, the polyampholyte physical gels without chemical crosslinkers will become an opaque strong gel with occurrence of microscopic phase separation[8,66,67]. Here, for the polyampholyte physical gels without any chemical crosslinkers, we deliberately tune the ionic bond strength at intermediate level by dialyzing against 2 M NaCl solution until the gels become transparent (Fig. 2e), so that the dissociation-association dynamical process can be easily realized for the ionic bonds with intermediate bond strength.

Data availability

All data generated in this study are provided in the main text and Supplementary Information. All data is available from the corresponding authors.

References

1. Zheng, N., Xu, Y., Zhao, Q. & Xie, T. Dynamic covalent polymer networks: A molecular platform for designing functions beyond chemical recycling and self-healing. *Chem. Rev.* **121**, 1716–1745 (2021).
2. Zhao, X. et al. Soft materials by design: Unconventional polymer networks give extreme properties. *Chem. Rev.* **121**, 4309–4372 (2021).
3. Samanta, S., Kim, S., Saito, T. & Sokolov, A. P. Polymers with dynamic bonds: Adaptive functional materials for a sustainable future. *J. Phys. Chem. B* **125**, 9389–9401 (2021).
4. Li, J. et al. Tough adhesives for diverse wet surfaces. *Science* **357**, 378–381 (2017).
5. English, A. M. et al. Programmable CRISPR-responsive smart materials. *Science* **365**, 780–785 (2019).
6. Zamani Alavijeh, R., Shokrollahi, P. & Barzin, J. A thermally and water activated shape memory gelatin physical hydrogel, with a gel point above the physiological temperature, for biomedical applications. *J. Mater. Chem. B* **5**, 2302–2314 (2017).
7. Taylor, L. D. & In Het Panhuis, M. Self-healing hydrogels. *Adv. Mater.* **28**, 9060–9093 (2016).
8. Sun, T. L. et al. Physical hydrogels composed of polyampholytes demonstrate high toughness and viscoelasticity. *Nat. Mater.* **12**, 932–937 (2013).
9. Yu, C. et al. Hydrogels as dynamic memory with forgetting ability. *Proc. Natl. Acad. Sci. USA* **117**, 18962–18968 (2020).
10. Kamata, H., Akagi, Y., Kayasuga-Kariya, Y., Chung, U.-I. & Sakai, T. "Nonswellable" hydrogel without mechanical hysteresis. *Science* **343**, 873–875 (2014).
11. Ducrot, E., Chen, Y., Bulters, M., Sijbesma, P. R. & Creton, C. Toughening elastomers with sacrificial bonds and watching them break. *Science* **344**, 186–189 (2014).
12. Larson, C. et al. Highly stretchable electroluminescent skin for optical signaling and tactile sensing. *Science* **351**, 1071–1074 (2016).
13. Matsuda, T., Kawakami, R., Namba, R., Nakajima, T. & Gong, J. P. Mechanoresponsive self-growing hydrogels inspired by muscle training. *Science* **363**, 504–508 (2019).

14. Chen, L. et al. A hyperelastic hydrogel with an ultralarge reversible biaxial strain. *Science* **383**, 1455–1461 (2024).
15. Israelachvili, J. & Pashley, R. The hydrophobic interaction is long range, decaying exponentially with distance. *Nature* **300**, 341–342 (1982).
16. Small, D. et al. Intermolecular π-to-π bonding between stacked aromatic dyads. Experimental and theoretical binding energies and near-IR optical transitions for phenalenyl radical/radical versus radical/cation dimerizations. *J. Am. Chem. Soc.* **126**, 13850–13858 (2004).
17. Daga, P. et al. Response of a Zn(ii)-based metal–organic coordination polymer towards trivalent metal ions (Al^{3+}, Fe^{3+} and Cr^{3+}) probed by spectroscopic methods. *Dalton Trans.* **50**, 7388–7399 (2021).
18. Seliktar, D. Designing cell-compatible hydrogels for biomedical applications. *Science* **336**, 1124–1128 (2012).
19. Cangialosi, A. et al. DNA sequence–directed shape change of photopatterned hydrogels via high-degree swelling. *Science* **357**, 1126–1130 (2017).
20. Freeman, R. et al. Reversible self-assembly of superstructured networks. *Science* **362**, 808–813 (2018).
21. Liu, J. et al. Bioresorbable shape-adaptive structures for ultrasonic monitoring of deep-tissue homeostasis. *Science* **383**, 1096–1103 (2024).
22. Djabourov, M., Nishinari, K. & Ross-Murphy, S. *Physical Gels from Biological and Synthetic Polymers*. (Cambridge University Press, Cambridge, 2013).
23. Zhou, H. X. & Pang, X. Electrostatic interactions in protein structure, folding, binding, and condensation. *Chem. Rev.* **118**, 1691–1741 (2018).
24. Yu, B., Pletka, C. C. & Iwahara, J. Quantifying and visualizing weak interactions between anions and proteins. *Proc. Natl. Acad. Sci. USA.* **118**, e2015879118 (2021).
25. Yu, B., Pettitt, B. M. & Iwahara, J. Dynamics of ionic interactions at protein–nucleic acid interfaces. *Acc. Chem. Res.* **53**, 1802–1810 (2020).
26. Han, C. C. & Akcasu, A. Z. *Scattering and Dynamics of Polymers: Seeking Order in Disordered Systems*. (Wiley, 2011).
27. Tanaka, T., Hocker, L. O. & Benedek, G. B. Spectrum of light scattered from a viscoelastic gel. *J. Chem. Phys.* **59**, 5151–5159 (1973).
28. Ilmain, F. & Candau, S. J. Cooperative diffusion in partially neutralized poly(acrylic acid) gels. *Makromolekulare Chemie. Macromol. Symp.* **30**, 119–131 (1989).
29. Joosten, J. G. H., McCarthy, J. L. & Pusey, P. N. Dynamic and static light scattering by aqueous polyacrylamide gels. *Macromolecules* **24**, 6690–6699 (1991).
30. Norisuye, T., Tran-Cong-Miyata, Q. & Shibayama, M. Dynamic inhomogeneities in polymer gels investigated by dynamic light scattering. *Macromolecules* **37**, 2944–2953 (2004).
31. Morozova, S. & Muthukumar, M. Elasticity at swelling equilibrium of ultrasoft polyelectrolyte gels: Comparisons of theory and experiments. *Macromolecules* **50**, 2456–2466 (2017).
32. Jia, D. & Muthukumar, M. Interplay between microscopic and macroscopic properties of charged hydrogels. *Macromolecules* **53**, 90–101 (2020).
33. Fang, L. & Brown, W. Dynamic light scattering by permanent gels: heterodyne and nonergodic medium methods of data evaluation. *Macromolecules* **25**, 6897–6903 (1992).
34. Geissler, E., Hecht, A. M., Rochas, C., Horkay, F. & Basser, P. J. Light, small angle neutron and X-ray scattering from gels. *Macromol. Symp.* **227**, 27–38 (2005).
35. Pusey, P. N. & Van Megen, W. Dynamic light scattering by nonergodic media. *Phys. A Stat. Mech. Appl.* **157**, 705–741 (1989).
36. Barrat, J. L., Joanny, J. F. & Pincus, P. On the scattering properties of polyelectrolyte gels. *J. Phys. II France* **2**, 1531–1544 (1992).
37. Jia, D. & Muthukumar, M. Effect of salt on the ordinary–extraordinary transition in solutions of charged macromolecules. *J. Am. Chem. Soc.* **141**, 5886–5896 (2019).
38. Muthukumar, M. Ordinary-extraordinary transition in dynamics of solutions of charged macromolecules. *Proc. Natl. Acad. Sci. USA.* **113**, 12627–12632 (2016).
39. Blake, C. C. F. et al. Structure of hen egg-white lysozyme: A three-dimensional Fourier synthesis at 2 Å resolution. *Nature* **206**, 757–761 (1965).
40. Yan, H. et al. Thermoreversible lysozyme hydrogels: Properties and an insight into the gelation pathway. *Soft Matter* **4**, 1313–1325 (2008).
41. Yan, H., Saiani, A., Gough, J. E. & Miller, A. F. Thermoreversible protein hydrogel as cell scaffold. *Biomacromolecules* **7**, 2776–2782 (2006).
42. Dixon, D. A., Dobbs, K. D. & Valentini, J. J. Amide-water and amide-amide hydrogen bond strengths. *J. Phys. Chem.* **98**, 13435–13439 (1994).
43. Spruijt, E., van den Berg, S. A., Cohen Stuart, M. A. & van der Gucht, J. Direct measurement of the strength of single ionic bonds between hydrated charges. *ACS Nano* **6**, 5297–5303 (2012).
44. Torrens, F. Calculation of partition coefficient and hydrophobic moment of the secondary structure of lysozyme. *J. Chromatogr. A* **908**, 215–221 (2001).
45. Raschke, T. M., Tsai, J. & Levitt, M. Quantification of the hydrophobic interaction by simulations of the aggregation of small hydrophobic solutes in water. *Proc. Natl. Acad. Sci. USA* **98**, 5965–5969 (2001).
46. Rubinstein, M. & Semenov, A. N. Thermoreversible gelation in solutions of associating polymers. 2. linear dynamics. *Macromolecules* **31**, 1386–1397 (1998).
47. Piazza, R. Polymer physics: Applications to molecular association and thermoreversible gelation. *Phys. Today* **65**, 56–57 (2012).
48. Leibler, L., Rubinstein, M. & Colby, R. H. Dynamics of reversible networks. *Macromolecules* **24**, 4701–4707 (1991).
49. Doi, M. & Edwards, S. F. *The Theory of Polymer Dynamics* (Clarendon Press, Oxford, 1986).
50. Muthukumar, M. *Physics of Charged Macromolecules: Synthetic and Biological Systems*. (Cambridge University Press, Cambridge, 2023).
51. Jia, D. & Muthukumar, M. Electrostatically driven topological freezing of polymer diffusion at intermediate confinements. *Phys. Rev. Lett.* **126**, 057802 (2021).
52. Jia, D. & Muthukumar, M. Dipole-driven interlude of mesomorphism in polyelectrolyte solutions. *Proc. Natl. Acad. Sci. USA* **119**, e2204163119 (2022).
53. McCoy, J. L. & Muthukumar, M. Dynamic light scattering studies of ionic and nonionic polymer gels with continuous and discontinuous volume transitions. *J. Polym. Sci. Pol. Phys.* **48**, 2193–2206 (2010).
54. Xing, Y. et al. Self-assembled DNA hydrogels with designable thermal and enzymatic responsiveness. *Adv. Mater.* **23**, 1117–1121 (2011).
55. Rockwood, D. N. et al. Materials fabrication from Bombyx mori silk fibroin. *Nat. Protoc.* **6**, 1612–1631 (2011).
56. Muthukumar, M. Dipole theory of polyzwitterion microgels and gels. *Gels* **10**, 393–415 (2024).
57. Nasto, A., Brun, P. T. & Hosoi, A. E. Viscous entrainment on hairy surfaces. *Phys. Rev. Fluids* **3**, 024002 (2018).
58. Nasto, A. et al. Air entrainment in hairy surfaces. *Phys. Rev. Fluids* **1**, 033905 (2016).
59. Tanaka, F. J. M. Theory of thermoreversible gelation. *Macromolecules* **22**, 1988–1994 (1989).
60. Semenov, A. N. & Rubinstein, M. J. M. Thermoreversible gelation in solutions of associative polymers. 1. *Macromolecules* **31**, 1373–1385 (1998).

61. Rubinstein, M. & Semenov, A. N. Dynamics of entangled solutions of associating polymers. *Macromolecules* **34**, 1058–1068 (2001).
62. González, A. E. Viscosity of ionomer gels. *Polymer* **24**, 77–80 (1983).
63. Sommer, J. U. On the dynamics of moderately crosslinked networks. *J. Chem. Phys.* **95**, 1316–1317 (1991).
64. Cieplak, M. & Muthukumar, M. Relaxation times of a random copolymer. *Macromolecules* **18**, 1350–1351 (1985).
65. Provencher, S. W. CONTIN: A general purpose constrained regularization program for inverting noisy linear algebraic and integral equations. *Comput. Phys. Commun.* **27**, 229–242 (1982).
66. Li, X. et al. Effect of salt on dynamic mechanical behaviors of polyampholyte hydrogels. *Macromolecules* **56**, 535–544 (2023).
67. Cui, K. et al. Phase separation behavior in tough and self-healing polyampholyte hydrogels. *Macromolecules* **53**, 5116–5126 (2020).

Acknowledgements

This work was supported by the National Key R&D Program of China (Grant No. 2023YFE0124500), the National Natural Science Foundation of China (Grant No. 22273114), the Strategic Priority Research Program of the Chinese Academy of Sciences (Grant No. XDB0770101), the National Key R&D Program of China (Grant No. 2023YFC2411203), and International Partnership Program of the Chinese Academy of Sciences (Grant No. 027GJHZ2022061FN). M.M. acknowledges support from the National Science Foundation (Grant No. DMR 2309539) and AFOSR (Grant No. FA9550-23–1-0584). We thank professor Mohan Srinivasarao from Georgia Institute of Technology for stimulating discussions.

Author contributions

D.J. conceived the idea and designed the project. Y.H.Z. performed the experiments. M.M. developed the theory and contributed to data analysis. D.J. and Y.H.Z. processed and analyzed most of the data. Y.S.J. synthesized silk fibroin gel and hyaluronic acid gel. Y.C.X. synthesized artificial mucus gel. Z.W.S. and Y.C.D. synthesized self-assembled DNA gel. M.M., D.J., and Y.H.Z. wrote and revised the paper. D.J. supervised the whole project.

Competing interests

The authors declare no competing interests.

Additional information

Supplementary information The online version contains supplementary material available at https://doi.org/10.1038/s41467-025-58571-2.

Correspondence and requests for materials should be addressed to Murugappan Muthukumar or Di Jia.

Peer review information *Nature Communications* thanks the anonymous reviewers for their contribution to the peer review of this work. A peer review file is available.